J Incl Phenom Macrocycl Chem (2016) 85:247–259
DOI 10.1007/s10847-016-0624-1

ORIGINAL ARTICLE

Physicochemical characterization and biological activities of the ethanol extract of *Bryophyllum pinnatum* (Lam.) Oken incorporated in β-cyclodextrin

Elisa G. Lanna[1] · Vanessa C. E. Bittencourt[2] · Ana Maria S. Moreira[2] · Jeferson G. Da Silva[2] · Orlando V. Sousa[1] · Ângelo M. L. Denadai[2]

Received: 20 September 2015 / Accepted: 10 May 2016 / Published online: 25 May 2016

Abstract In the present work, a phytocomplex formed by ethanol extract of *Bryophyllum pinnatum* (Lam.) Oken (EEBP) and β-cyclodextrin (βCD) has been prepared at weight proportion of 1:1, characterized through several physical chemistry methods, and incorporated in an oil-in-water emulsion in order to evaluate its topical anti-inflammatory effect. Changes in the spectra of infrared and UV/VIS as well as TGA and DTA curves suggested the existence of interactions between components of extract and βCD. The incorporation of βCD to the extract also promoted an increase in the zeta potential of the aggregates spontaneously formed in water, with consequent reduction of their size. The in vitro antioxidant activity was also evaluated, showing an improvement of the radical-scavenging ability in presence of βCD. Finally, the topical application of EEBP/βCD semi-solid formulation significantly inhibited the ear edema induced by Croton oil if compared with free EEBP, justifying the use of phytotherapic formulation based on *B. pinnatum* as a remedy for skin disorders.

Keywords *Bryophyllum pinnatum* · Cyclodextrin · Phytocomplex · Anti-oxidant · Anti-inflammatory · Flavonoids

Introduction

In the last decades, many research groups and pharmaceutical companies in the whole world have improving their technologies based on the guiding principles of green chemistry, aiming to minimize the use of potentially hazardous substances in production of drugs, reduce the generation of waste and operate in other environmentally friendly ways. In this context, the natural products represent an appropriate alternative on the synthetic therapeutic arsenal and play an important role due to the synergic effects among the different constituents [1].

In the field of phytotherapy, the effectiveness of many species of medicinal plants depends on the appropriate delivery of active compounds in desired target. Under this aspect, the poor bioavailability together with low solubility in water and the short chemical stability related to physicochemical factors, such as pH, temperature and light, have restricted the application of natural compounds as pharmaceutical products. Thus, the preservation of the structural integrity of bioactive molecules requires many times the use of excipients and/or incorporation in a finishing formulation with the capacity to deliver them to the physiological targets without losing any bioactivity [2–6].

In order to improve the bioavailability and ensure the synergism among the active constituents of extracts, the combination of herbal medicine with nanotechnological devices has been proposed. In this combination, the nanostructured systems might be able to potentiate the

Electronic supplementary material The online version of this article (doi:10.1007/s10847-016-0624-1) contains supplementary material, which is available to authorized users.

✉ Ângelo M. L. Denadai
angelo.denadai@ufjf.edu.br

[1] Faculdade de Farmácia, Universidade Federal de Juiz de Fora (UFJF), Campus Juiz de Fora, Rua José Lourenço Kelmer, s/n - Campus Universitário, Bairro São Pedro, Juiz de Fora, MG 36036-900, Brazil

[2] Departamento de Farmácia, Universidade Federal de Juiz de Fora (UFJF), Campus Governador Valadares, Av. Dr. Raimundo Monteiro de Rezende, 330, Centro, Governador Valadares, MG 35010-177, Brazil

action of bioactive molecules with reduction of required dose and side effects [1, 5, 6].

Actually, there are several methods to enhance the bioavailability of natural extracts. For this purpose, their association with cyclodextrins seems to be very promising when compared with other methods, due to the possibility of formation of inclusion compounds with components of extract—phytocomplexes. They can deliver small molecules at sufficient concentration during the entire treatment period and directed to the desired site of action.

Cyclodextrins are macrocyclic, non reducing maltooligosaccharides composed of glucose units linked by α-(1,4) glycosidic bonds. The most common cyclodextrins are α-, β- and γ-cyclodextrin, which are composed of six, seven and eight glucopyranose units, respectively. The size of cyclodextrin cavity allows selectivity for the complexation of guest molecules, and, therefore, they have the ability to form inclusion complexes stabilized by non-covalent interactions with a wide variety of compounds [7–11].

Microencapsulation in β-cyclodextrin (βCD) has been successfully applied with isolated plant bioactive compounds, such as alkaloids [12], phenolic acids [13, 14], polyphenolics compounds [15, 16] as well as complex mixtures, like olive leaf extract [3], propolis balsam [17], hibiscus anthocyanins-rich extract [4], flavonoid-rich extract [5], which improved different biological activities.

Bryophyllum pinnatum (Lam.) Oken (BP), known in Brazil as "Folha da Fortuna", is a native plant from Madagascar belonging to Crassulaceae family, which has been found throughout the hot and moist parts of Asia, Australia, New Zealand, Africa, and America. The leaves are widely used in traditional medicine due to their biological activities for the treatment of several diseases, including inflammation and oxidative processes [18–20].

In a recent paper, it was demonstrated that the ethanol extract of BP (EEBP) leaves presented a marked anti-inflammatory effect in acute and chronic cutaneous inflammation. This activity was ascribed to the action of flavonoids in inhibition of different inflammatory targets, especially the arachidonic acid pathway, justifying its traditional use as a remedy for skin disorders [21].

Various substances have been isolated and identified in different extracts and fractions of BP such as phenols, phenyl propanoids, flavonoids, triterpenoids, steroids, saponins and alkaloids [19, 22, 23]. Considering that several of these substances are thermo or photosensible, and based on the fact that there are many studies about the improvement of biological activity of plant extracts by cyclodextrins, the main objective of this work was to describe a new semi-solid formulation constituted by phytocomplex of the ethanol extract of BP leaves with βCD (EEBP/βCD).

Initially the EEBP/βCD phytocomplex was obtained by co-precipitation method combined with lyophilization. Afterwards, it was studied using UV/VIS and FTIR spectroscopies, dynamic light scattering (DLS), zeta potential (ZP), thermogravimetric analysis (TGA) and differential thermal analysis (DTA). In addition, the antioxidant activity of EEBP and EEBP/βCD phytocomplex were evaluated using two different assays (2,2-diphenyl-1-picrylhydrazyl (DPPH) radical scavenging method and ferric reducing antioxidant power (FRAP) assay. Finally, the topical anti-inflammatory effect of the semi-solid formulation of EEBP/βCD was evaluated by acute mice ear edema induced by Croton oil, measuring the ear weight and myeloperoxidase (MPO) activity, followed by histopathological analyses of ear tissue samples sensitized with Croton oil.

Materials and methods

Plant material

Bryophyllum pinnatum (Lam.) Oken was cultivated and collected in Juiz de Fora, Minas Gerais State, Southeast region of Brazil (21°46′10, 46013″S and 43°21′49, 88313″W), in May 2014. The species was identified by Dra. Fátima Regina Gonçálves Salimena and a voucher specimen (CESJ Number 46575) was deposited in the Herbarium of the Federal University of Juiz de Fora, Brazil.

Extract preparation

Dried and powdered leaves (500 g) were exhaustively extracted with ethanol (1.5 L) by static maceration at room temperature every 48 h for 20 times. The ethanol extract (EEBP) was filtered and evaporated under a rotary vacuum evaporator at controlled temperature (50–60 °C). This product was placed in a desiccator with silica to yield 83 g of extract (16.7 %).

Preparation of the phytocomplex

The phytocomplex formed between EEBP with βCD (EEBP/βCD) was prepared by coprecipitation method [24–26]. Briefly, 1.0 g of EEBP and 1.0 of βCD were dissolved into 50 mL of 1:1 (v/v) ethanol/water mixture. This solution was stirred and hold upon heating at ≈50 °C during 24 h and then submitted to the freeze-drying process to achieve the solid phytocomplex.

Differential thermal analysis (DTA) and thermogravimetric analysis (TGA)

Differential thermal analysis (DTA) and thermogravimetric analysis (TGA) were performed using TGA/DTA modulus STA7200RV from HITACHI, coupled to a photo visualization system. Data were recorded for EEBP, βCD, EEBP/βCD and physical mixture (PM) at weight ratio of 1:1. The experiments were carried out using a dynamic air atmosphere of 50 mL/min, a heating rate of 10 °C/min, and sensitivity of 1.0 °C. For each experiment, it was used approximately 5 mg of sample, which was placed in open pans of platinum.

Spectroscopic characterization

UV–Vis absorption spectra were recorded in a PerkinElmer UV–Vis double beam spectrophotometer, model Lambda 25, equipped with a PC for data processing (Software: UV–Win Lab®, from PerkinElmer), in spectral range of 190–700 nm. The spectra were recorded at 25 °C using a peltier device for control of temperature. Samples for UV–Vis experiment were prepared by initial dissolution of 2 mg of EEBP or 4 mg of EEBP/βCD phytocomplex in 0.5 mL of ethanol, followed by dilution in milli Q® water up to final volume of 25.0 mL (2 % of ethanol v/v). In order to guarantee the same extract concentration in both samples, the final concentrations obtained were 80 and 160 μg/mL for EEBP and EEBP/βCD solutions, respectively. Distilled water containing the same concentration of ethanol was used as blank. Quartz cells of 3 mL and 1 cm of optical path were used in the experiments.

The FTIR-ATR spectra of the samples were carried out between 4000 and 450 cm^{-1} using a Perkin Elmer Spectrum Two™, FTIR spectrometer coupled with PIKE Attenuated Total Reflectance accessory (ATR). The samples were directly applied on diamond surface of ATR modulus and the spectra were recorded as the average of 16 scans with spectral resolution of 2 cm^{-1}. For the treatment of the spectra, it was used the Perkin Elmer Spectrum ES software (version 10.03.08.0133).

Hydrodynamic diameter

A Malvern Zetasizer Nano ZS particle analyzer using polyethylene square cells was employed to measure the average hydrodynamic diameter (D_h) of EEBP and EEBP/βCD phytocomplex by dynamic light scattering. The same solutions used in UV–vis experiment were subjected to a monochromatic light (4 mW He–Ne laser, wavelength 633 nm) and the scattered light intensity was measured at an angle of 90°. The hydrodynamic diameters were determined by the average of five independent measurements, each of them obtained as the mean of 30 counts.

Zeta potential and electrical conductivity

Zeta potential (ZP) and electrical conductivity experiments were also performed using the Malvern Zetasizer Nano ZS equipment. The ZP was determined by means of the Laser Doppler Micro-electrophoresis technique, at scattering angle of 173° [27], using a disposable cell folded capillary (DPS1060). The ZP values were calculated as the average of ten independent measurements, each of them obtained as the mean of 30 counts. The same solutions used in UV–vis experiments were also used here.

Preparation of the semi-solid formulations

The βCD, EEBP and EEBP/βCD phytocomplex were incorporated into an oil-in-water anionic emulsion (AE) designed for topical administration. Both phases of AE were obtained separately by mixing the ingredients at 75 °C for 30 min. Oil phase was added dropwise to the water phase upon agitation in order to obtain the emulsion. Excipients amounts used for preparation of AE are shown in Table S1 in Supplementary Material.

For preparation of the semi-solid formulations, βCD, EEBP or EEBP/βCD phytocomplex were initially suspended in 1.0 mL of propyleneglycol and then incorporated into emulsions at the following concentrations: 0.05, 0.125 and 0.25 % for βCD and EEBP, and 0.1, 0.25 and 0.5 % for EEBP/βCD. The amount of EEBP was the same in the AE + EEBP and AE + EEBP/βCD samples.

Rheological characterization

Rheological behavior of the formulations (AE, AE + βCD, AE + EEBP and AE + EEBP/βCD) was investigated through the steady flow rheometry in a controlled shear rate rheometer R-180 from Prorheo®, using the DIN standard 53 019 measuring system, which consist of a cup (d = 26.03 mm, V = 25 mL) and a bob (d = 24.00 mm, h = 36.00 mm). The samples were pre-sheared by 2 min and then they were subjected to a cyclical variation of shear rate: from 100 to 1000 s^{-1} and from 1000 to 100 s^{-1}. The shear rate was varied in 20 linearly spaced steps what took 30 s to be completed. The data were initially handled by using the software RHESY from Prorheo® and subsequently, they were exported to the compatible format for Microcal Origin® 7.0. The measurements were performed at 30 °C using an external thermostatic bath.

Antioxidant Assays

The antioxidant activity of EEBP and EEBP/βCD phytocomplex was determined by two methods, namely DPPH—radical scavenging capacity and FRAP—ferric reducing power, following the procedures described by Mensor et al. [28] and Oyaizy [29, 30], respectively. Experiments were performed in triplicate and rutin was used as positive control.

Determination of antioxidant activity by the scavenging of the stable radical DPPH·

For the calculus of the percentage of the radical scavenging activity (%RSA), the following solutions were prepared: (1) samples solution—by mixing of 2.5 mL of the sample in the desired concentration with 1 mL of DPPH solution (0.3 mM); (2) blank sample solution—by mixing of 2.5 mL of the sample in the desired concentration with 1 mL of solvent; (3) control solution—by mixing of 2.5 mL of solvent with 1 mL of DPPH solution (0.3 mM); and (4) blank control solution—only the solvent. In all cases, 90 % (v/v) ethanol/water solution was used as solvent. After incubation of 30 min in the dark and at room temperature, the absorbance of solutions was measured at 515 nm in a spectrophotometer (SHIMADZU®, UV-1800). The %RSA was calculated by the following equation:

$$\%\,RSA = 100 - \left[\left(\frac{Abs_{sample} - Abs_{blanksample}}{Abs_{control} - Abs_{negativecontrol}}\right) \times 100\right] \quad (1)$$

The EEBP and EEBP/βCD solutions were prepared in the concentration range from 1 to 750 μg/mL and the rutin solution was prepared in the concentration range from 1 to 30 μg/mL. The IC_{50} value for each sample, defined as the antioxidant concentration required to scavenge 50 % of the free radicals present, was calculated from the nonlinear regression curve of Log concentration of the test extract (μg/mL) against the mean percentage of the radical scavenging activity [28].

Determination of antioxidant activity by the ferric ion reducing antioxidant power (FRAP)

For this experiment, 1 mL of each sample was mixed with 2.5 mL of phosphate buffer (200 μM, pH 6.6) and 2.5 mL of 1 % potassium ferricyanide. The mixtures were incubated for 20 min at 50 °C. At the end of the incubation, 2.5 mL of 10 % trichloroacetic acid was added to the mixtures and centrifuged at 3000 rpm for 8 min. The upper layer (2.5 mL) was mixed with 2.5 mL of distilled water and 0.5 mL of 0.1 % ferric chloride. The absorbance was measured at 700 nm spectrophotometer (SHIMADZU®, UV-1800). The blank solution was prepared by substituting 1 mL of sample for 1 mL of distilled water. IC_{50} (50 % inhibitory concentration) values (μg/mL) were calculated and indicated the inhibitory concentration at which the absorbance was 0.5 for reducing power.

Anti-inflammatory assay

Animals

Male Swiss albino mice (*Mus musculus*) (45–55 days) weighting 25–30 g were used in the experiments. The animals were provided by the Central Biotery of the Federal University of Juiz de Fora. After acquisition, the animals were grouped and housed in plastic cages ($47 \times 34 \times 18$ cm^3) under a 12 h light/12 h dark cycle at room temperature (22 ± 2 °C), received balanced feed Nuvilab Rodents (Nuvital Nutrients, Colombo, Brazil) and had free access to water. Animal care and the experimental protocol followed the principles and guidelines suggested by the Brazilian College of Animal Experimentation (COBEA) and the EC Directive 86/609/EEC for animal experiments. Experiments were approved by the local Ethical Committee (Protocol Number 105/2012).

Croton oil single application-induced mice ear edema

Croton oil-induced ear edema in mice was performed according to the method described by Schiantarelli et al. [31]. Ear edema was induced (n = 7/group) by topical application of 20 mL of Croton oil 2.5 % (v/v) in acetone on the inner surface of the right ear, while the left ear received 20 mL of acetone (vehicle). After 15 min, semi-solid formulation with EEBP (AE + EEBP) (0.05, 0.125 and 0.25 %), semi-solid formulation with EEBP/βCD (AE + EEBP/βCD) (0.1, 0.25 and 0.5 %) and dexamethasone (0.1 % as positive control) were topically applied on the right ear. The negative control group received 20 μL of acetone on the right ear. The ear edema was evaluated 6 h after Croton oil application and measured by the difference of weight (mg) between right and left (non-inflamed) ears. For this, the animals were euthanized with overdose of ketamine and xylazine and ear tissue samples (6 mm diameter) were collected of each animal using a metallic punch (Richter, São Paulo, SP, Brazil). After weighing, ear tissue samples (6 mm) were conserved in 10 % formaldehyde (v/v) and submitted to histopathological analysis.

Leukocyte infiltration markers

The inflammatory cell infiltration in the edematous mouse ear was estimated by myeloperoxidase (MPO) activities, a neutrophil marker [32]. The method of Bradley et al. [33] modified by Deyoung et al. [32] was used in order to evaluate the enzymatic activity. Firstly, the samples were homogenized in phosphate buffer (80 mM, pH 5.4) containing 0.5 % HTAB and centrifuged at 3.000 rpm at 4 °C for 10 min, and the supernatant was removed. For the MPO activity measurement, 25 µL of supernatant was added to 25 µL of 3,3′,5,5′-tetramethyl-benzidine (1.6 mM) in DMSO, 100 µL of 0.003 % H_2O_2 v/v in phosphate buffer (0.08 M, pH 5.4) in a 96-well plate and incubated at 37 °C for 5 min, to start the reaction. To stop the reaction, the microplates were incubated in an ice bath a 4 °C, and 100 µL of sulfuric acid was added. The absorbance of all reactions was measured in a Thermoplate TR-Reader® microplate reader and the coloration intensities were assessed at 450 nm. The values are expressed as optical densities, corrected for the protein content, which was measured by the method of Lowry et al. [34] and Sargent et al. [35]. Experiments were done in triplicate.

Histopathological analysis

Ear tissue samples preserved in formaldehyde 10 % (v/v) were fixed in 70 % ethanol for 24 h. Subsequently, the tissues were dehydrated, blocked in paraffin and then sectioned with a microtome (5 mm) (TBS Cut 4060 Rotary Microtome, Thermo Fisher Scientific Inc., Pittsburgh, PA). The transverse sections were stained with hematoxylin and eosin (H&E) for the evaluation of edema (dermis) thickness, epidermal hyperplasia, inflammatory cells infiltration and vasodilation. Representative areas were selected for qualitative light microscopic analysis (BX 51 Olympus microscopy, Olympus Optical Co., LTD, Hatagaya, Shibuya-ku, Tokyo, Japan; magnification: 200×) and images were captured (photomicrograph) through the Image-Pros Plus software (version 6.0, Media Cybernetics, Inc., USA), which was also used to acquire measurements of ear thickness (mm) of tissue samples. A representative section from each group of animals was selected to show the histopathological changes. The measurements were made at five different points of each section and each group was represented by four section (n = 4).

Statistical analysis

Data were expressed as mean ± S.E.M. Statistical significance was analyzed by the one-way analysis of variance (ANOVA) followed by the Student Newman-Keuls test as post hoc. *P* values below 0.05 were considered significant.

Results and discussion

Spectroscopic characterization of inclusion complex

The FTIR spectra of βCD, EEBP and EEBP/βCD phytocomplex are displayed in Fig. 1, which were used to verify the formation of interactions between βCD with components of the extract. The βCD spectrum is in accordance with those previously described in literature, with main absorptions at 3391, 2929, 1157, 1179, 1022 and 941 cm^{-1}, which correspond to the symmetric and antisymmetric stretching of ν[OH], ν[CH_2], ν[C–C], bending vibration of ν[O–H] and the skeletal vibration involving (α-1,4 linkage), respectively [36].

The EEBP spectrum showed bands at 1039, 1610, 1736, 2855-2922 and 3305 cm^{-1} that can be associated to the stretching of C–O, C=C (aromatic), C=O, C–H and O–H bonds, respectively [37–39]. Moreover, the range between 900 and 1130 cm^{-1} was similar to those observed in FTIR spectra of compounds containing glucopyranosyl units, even suggesting the existence of glycosylated flavonoids in the components of extract [36].

In the EEBP/βCD spectrum, significant changes in the shape and position of the vibrational bands were observed, as result of interactions between extract components with the βCD. The EEBP bands at 1039, 1371 and 1313 cm^{-1} were shifted towards 1023, 1358 and 1301 cm^{-1} respectively, while the bands at 924, 1707, 1600, 1517, and 3305 cm^{-1} had their intensity reduced or disappear. These changes were ascribed to be due to the vibrational restriction of molecules upon inclusion or association with βCD.

The UV–Vis spectroscopy was used in order to verify the existence of interactions in solution. In the spectrum of the EEBP (Fig. 2a), it can be observed four main bands at 269, 374, 400 and 670 nm. The band at 269 nm was associated with the absorption involving the A-ring

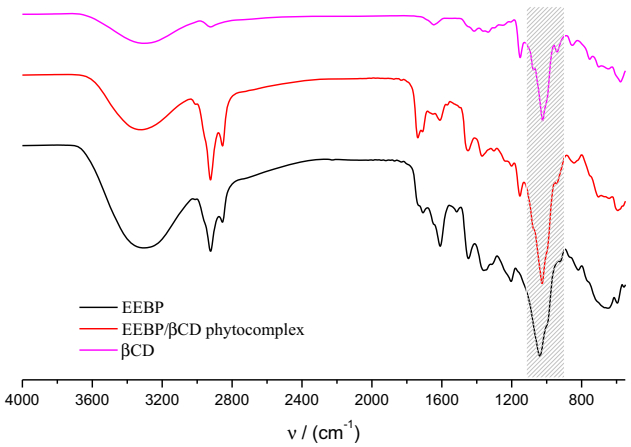

Fig. 1 ATR infrared spectra of βCD, EEBP, and EEBP/βCD phytocomplex

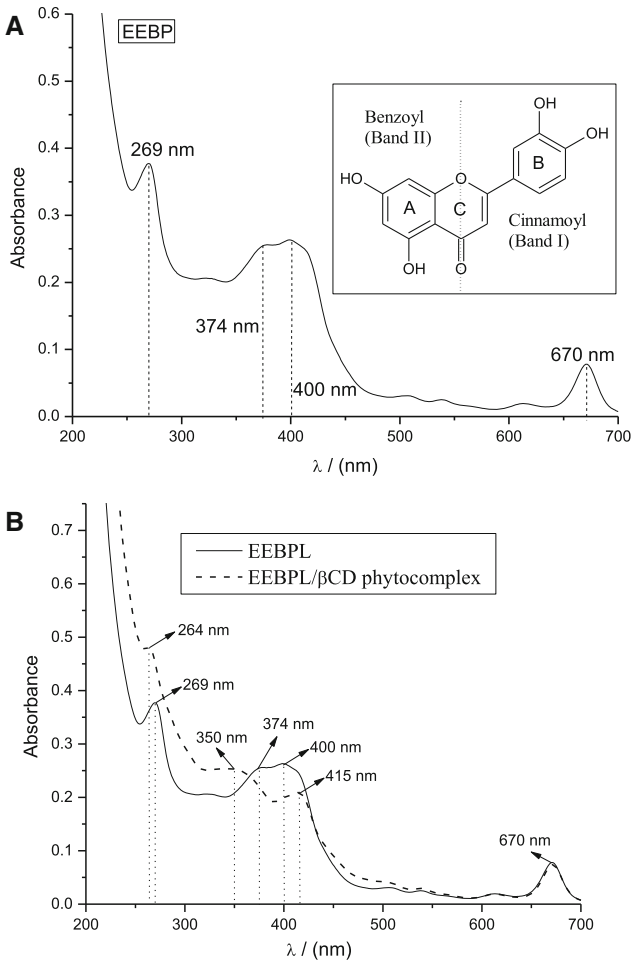

Fig. 2 **a** UV–Vis spectra of EEBP with attributions of bands of the main chromophores and **b** comparative UV–Vis spectra of EEBP and EEBP/βCD phytocomplex

benzoyl system of flavonoids (band II) while the band at 374 nm was associated with B-ring absorption of cinnamoyl system of flavonoids (band I) [21, 40]. The bands at 400 and 670 nm were associated with chlorophylls [41].

Figure 2b illustrates a comparison between the UV–Vis spectra of EEBP and EEBP/βCD phytocomplex where can be observed clear changes in the presence of βCD. A hypsochromic shift of band II was observed from 269 to 264 nm while a sharp change was observed in the range of 300–400 nm. These modifications suggest interactions between βCD and chromophore groups from flavonoids. However, it is not possible to verify interaction with chlorophyll in this case, due to no change in the band at 670 nm.

Differential thermal analysis (DTA) and Thermogravimetric analysis (TGA)

TGA combined with DTA represent important analytical tools to investigate the thermal stability of inclusion complexes [10, 42, 43]. In the Fig. 3a and b are shown the DTA and TGA curves for EEBP, βCD, EEBP/βCD and PM, obtained in dynamic atmosphere of air, in the range of 25–300 °C. The complete curves, in the range between 25 and 800 °C, are presented in the Figure S1 of Supplementary material.

As can be seen in Fig. 3a, βCD showed a loss of mass of ≈16 % in the range 70–115 °C, corresponding to the releasing of approximately twelve water molecules. In the DTA curve, it was observed an endothermic peak started at ≈70 °C, with a maximum at 95 °C, confirming the dehydration. After this event, it remained stable until ≈280 °C, when begins its decomposition [44].

In the TGA curve for EEBP, it was observed a thermal stability of the extract until ≈95 °C. Through photovisualization system (see video data 1 in supplementary material), it was possible to observe that the extract forms a

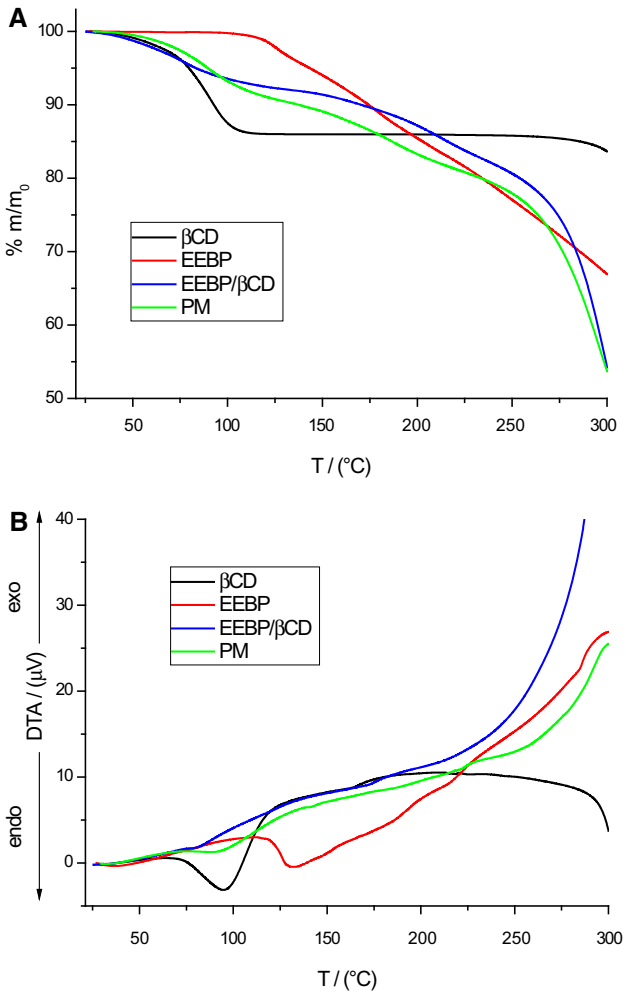

Fig. 3 **a** TGA curves and **b** DTA curves for βCD, EEBP, EEBP/βCD and PM at weight ratio 1:1. Experiments were performed in dynamic atmosphere of air. The overall curves in the range from 25 to 800 °C are shown in supplementary material (Fig. S1)

molten mixture at around 100 °C followed by consecutive thermal decomposition stages until 586 °C, when occurs the calcination of the material.

Different from the EEPB, the EEBP/βCD phytocomplex lost ≈8 % of its mass up to 128 °C. This event was attributed to the releasing of remaining water molecules present in the phytocomplex, once it occurred at the same temperature of dehydration of βCD. Through video data 2 (available in supplementary material), it was possible to visualize that within this range of temperature did not occur the fusion of the phytocomplex, as result of interaction between EEBP with βCD. Moreover, interactions of EBPP components with βCD caused a sharp attenuation in the DTA curve in the range between 100 and 200 °C. After 250 °C, a strong exothermic peak in DTA curve was observed, matching with decomposition of βCD.

The DTA and TGA curves for PM did not overlap the EEBP/βCD curves, indicating also that in presence of βCD there are intermolecular interactions resulting from the contact of the components during the preparation of the samples, which alter the thermal stability of the material.

Colloidal characterization of EBPP and EBPP/βCD phytocomplex in ethanol/water mixture

In order to assess the ability of βCD modulate the self-aggregation of EEBP and EEBP/βCD in water/ethanol mixture (98:2 v/v), the colloidal properties of the so-formed aggregates were investigated by measurements of electrical conductivity (κ), average hydrodynamic diameter $\langle D_h \rangle$ and zeta potential (ZP).

Figure 4a shows the average $\langle D_h \rangle$ for the two suspensions, where it can be observed the presence of nanometric structures resulting from self-aggregation of the extract components. In presence of βCD, a sharp reduction of size of the assemblies was observed, confirming the modulating effect of βCD on particles size. A possible mechanism involved in the reduction of size is the partial solubilization of extract components with subsequent formation of inclusion compounds [45].

Electrical conductivity was used to evaluate the ionization profile of the above described samples, since the presence of ions in solution helps to stabilize nanostructures through adsorption in their surfaces [46]. From Fig. 4b, it can be seen that the electrical conductivity of the EEBP/βCD solution increased significantly in relation to the EBPP solution. This change was attributed to the partial ionization of the βCD, with consequent releasing of H^+ ions to the aqueous environment and transference of ionic species from aggregates to solution.

The last step of the colloidal characterization was accomplished by zeta potential measurement, which is a measurement of the electrostatic energy on surface of

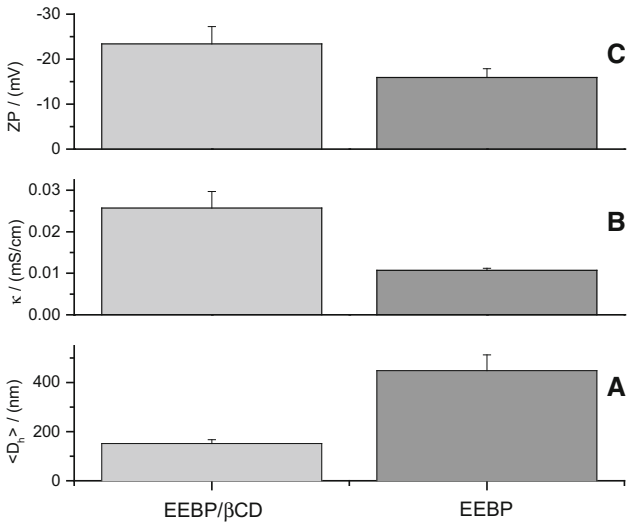

Fig. 4 Colloidal characterization of EEBP (80 μg/mL) and EBPP/βCD (160 μg/mL) aqueous solutions by **a** hydrodynamic diameter measurement by DLS, **b** electrical conductivity and **c** zeta potential at 25 °C

particles (Fig. 4c). In this case, negative ZP values are found for the both EEBP and EEBP/βCD aggregates, indicating the existence of negative charges on the particles surface. These results comply with the higher electrical conductivity values found for EEBP/βCD phytocomplex, suggesting therefore a greater degree of ionic adsorption, which contributes to increase the electric repulsion between the particles and hinder the coalescence and the growing of the particles. Moreover, the more negative ZP values for EEBP/βCD might be resultant from the localization of ionized cyclodextrins at nanoassemblies surface. The numeric data of Fig. 4 is also showed in Table S2 in supplementary material.

Antioxidant effect of EEBP and EEBP/βCD phytocomplex

The presence of flavonoids containing phenolic OH groups confers to the *B. pinnatum* extracts antioxidant profile [21]. Thus, the antioxidant activities of EEBP and EEBP/βCD phytocomplex were evaluated by using two electrons transfer reactions, each of them using different chromogenic redox reagents with different standard potentials. The first one was the 2,2-diphenyl-1-picrylhydrazyl radical scavenging capacity (DPPH-SC) and the second one was the ferric ion reducing antioxidant power (FRAP), both assays were monitored spectrophotometrically.

For the both experiments, the association between EEBP and βCD improved significantly ($P < 0.05$) the antioxidant activity of phytocomplex when compared with EBPP. In DPPH-SC assay, the IC_{50} value of EEBP for DPPH radicals was 12.27 ± 0.38 μg/mL, while for EEBP/βCD

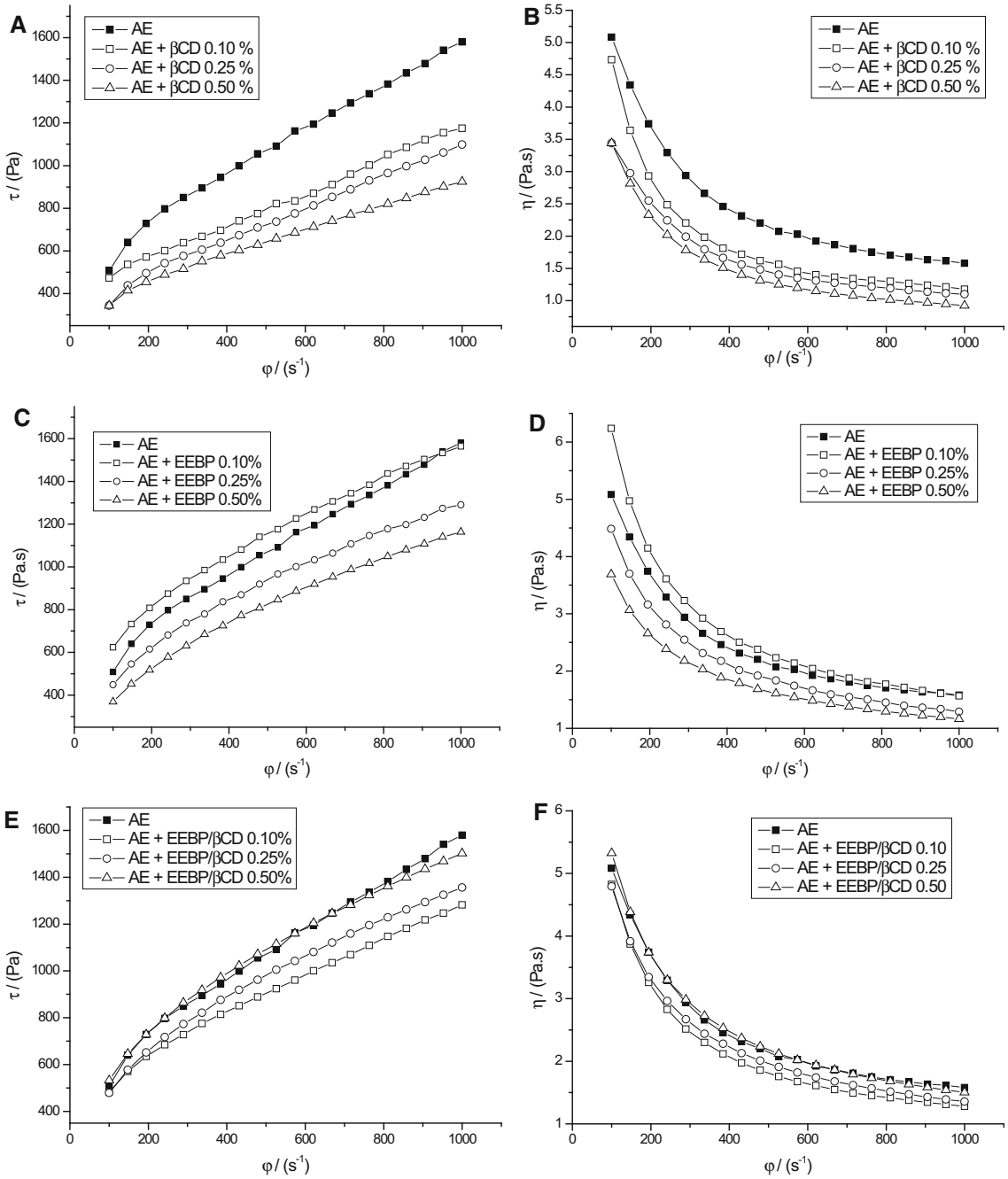

Fig. 5 Flow and viscosity curves for different concentrations of **a** AE + βCD, **b** AE + EBPP and **c** AE + EEBP/βCD. Experiments performed with loop of shear rate varied from 100 to 1000 s^{-1}, and vice versa, at 30 °C

phytocomplex was only 7.03 ± 0.92 μg/mL. Rutin appeared to be a strong DPPH scavenging agent with an IC_{50} value of 8.37 ± 0.23 μg/mL. The DPPH radical-scavenging ability of an antioxidant is thought to be closely associated with its hydrogen-donating ability [47]. Thus, when βCD is conjugated with EBPP, one or several hydrogen bonds can be formed between −OH of the polyphenols constituents of EEBP with the oxygen atoms of the cyclodextrins. These hydrogen bonds would weaken the covalent bonds between hydrogen and oxygen in the hydroxyl groups, which in turn would make the hydrogen donation easier.

When antioxidant activity was evaluated by the FRAP method, EEBP/βCD phytocomplex also showed a strongest antioxidant activity (IC_{50} = 387.21 ± 1.12 μg/mL) in comparison with EEBP (IC_{50} = 536.90 ± 1.69 μg/mL). Rutin appeared to have a strong antioxidant activity with an IC_{50} value of 206.7 ± 1.1 μg/mL. According to

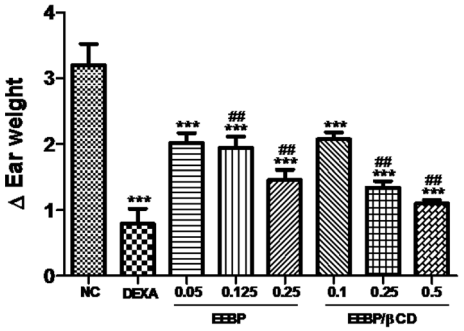

Fig. 6 Topical effect of formulations containing EEBP (0.05, 0.125 and 0.25 % w/w) and EEBP/βCD (0.1, 0.25 and 0.5 % w/w), on Croton oil induced mice ear edema. Dexamethasone at 0.1 % w/w was used as positive control and 20 μL of acetone as negative control. After 6 h of challenge, the ear edema was evaluated based on the increase in ear weight (ΔEar weight/mg), obtained by the difference between the right ear (inflamed) and the left ear (non-inflamed). The bars represent the mean ± SEM (n = 7). $^{***}P < 0.001$ represents the significance level when formulations were compared with negative control group. $^{\#\#}P < 0.01$ represents the significance level when EBPP and EBPP/βCD groups were compared among them. ANOVA followed by Student–Newman–Keuls test as post hoc

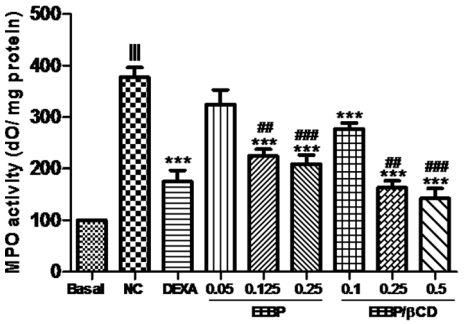

Fig. 7 Effect of EEBP (0.05, 0.125 and 0.25 % w/w), and EEBP/βCD (0.1, 0.25 and 0.5 % w/w) formulations on MPO activity induced by Croton oil. DEXA 0.1 % w/w was used as positive control and 20 μL of acetone as negative control. MPO activity determined after 6 h of challenge. The bars represent the mean ± S.E.M (n = 6). $^{III}P < 0.001$ represents the significance level when compared with basal (group without inflammation). $^{***}P < 0.001$ represents the significance level when compared with negative control group. $^{\#\#}P < 0.01$ and $^{\#\#\#}P < 0.001$ represents the significance level when EBPP and EBPP/βCD groups were compared among them. ANOVA followed by Student–Newman–Keuls test as post hoc

Lue et al. [48], the hydrophobic compounds may not be readily accessible in an aqueous system for the reduction of ferric ions. Since this assay was carried out in an aqueous solution, the aqueous solubility of the antioxidant being tested would be expected to have an effect on the outcome. Thus, the increase in ferric reducing power of EEBP/βCD was likely related to the improvement in its solubility.

Rheological characterization of the topical formulation

Rheological studies permit to gather several information about emulsions and predict their performances during production and after application. From Fig. 5a–f it is possible to observe the shear stress (τ) and viscosity (η) variations due to the increasing and decreasing shear rate (φ) applied during the rheological tests on formulations.

In general, the results obtained show that all emulsions can be considered pseudoplastic (nonNewtonian) fluids because their τ values were not linear with φ and because η reduced upon applied shear rate. The explanation for this behavior is given in terms of the destruction of colloidal aggregates of the components of Lanette (higher fatty alcohols and alkyl sulfates) by the application of shearing. The highest reduction in viscosity (approximately 50 %) occurred up to $\varphi \approx 400\ s^{-1}$. Above this value, the fluids reached the steady state and therefore the changes in viscosity were low for all studied conditions.

These data suggest that the optimum shear rate for processing the sample is around $400\ s^{-1}$, which in turn is a typical value for industrial operations, such as mixing, stirring, transportation in pipelines and spraying fluid onto superficies [49]. On the other hand, it would be expected that at rest or at very low shear rate (storage condition), the fluid would exhibits very large viscosity.

According to the Fig. 5a–f, the dissolution of βCD, EBPP and EBPP/βCD phytocomplex in AE caused different effects on viscosity of formulations as result of different mechanisms of interactions between solutes with components of emulsion. In presence of βCD (Fig. 5a, b), both τ and η values reduced with increase of βCD concentration. For AE + EBPP system, the behavior was similar. Increasing concentration of EBPP also caused reduction of τ and η values (Figs. 5c, d). It is believed that βCD and EBPP components act to favor of the breakdown of nanostructures present in Lanette, increasing therefore the fluidity of the cream.

Regarding the formulations containing EEBP/βCD at 0.1 % (Fig. 5e, f), it can be observed that dissolution of phytocomplex in the anionic matrix caused an initial drop in both τ and η values. However, as the EBPP/βCD concentration is increased, the shear stress and viscosity values returns to the initial values, suggesting the existence of a compensatory effect on rheological properties as the concentration is increased.

Anti-inflammatory activity of the topical formulation

Mice ear edema is a well-established model of acute inflammation that has been used in the investigation of

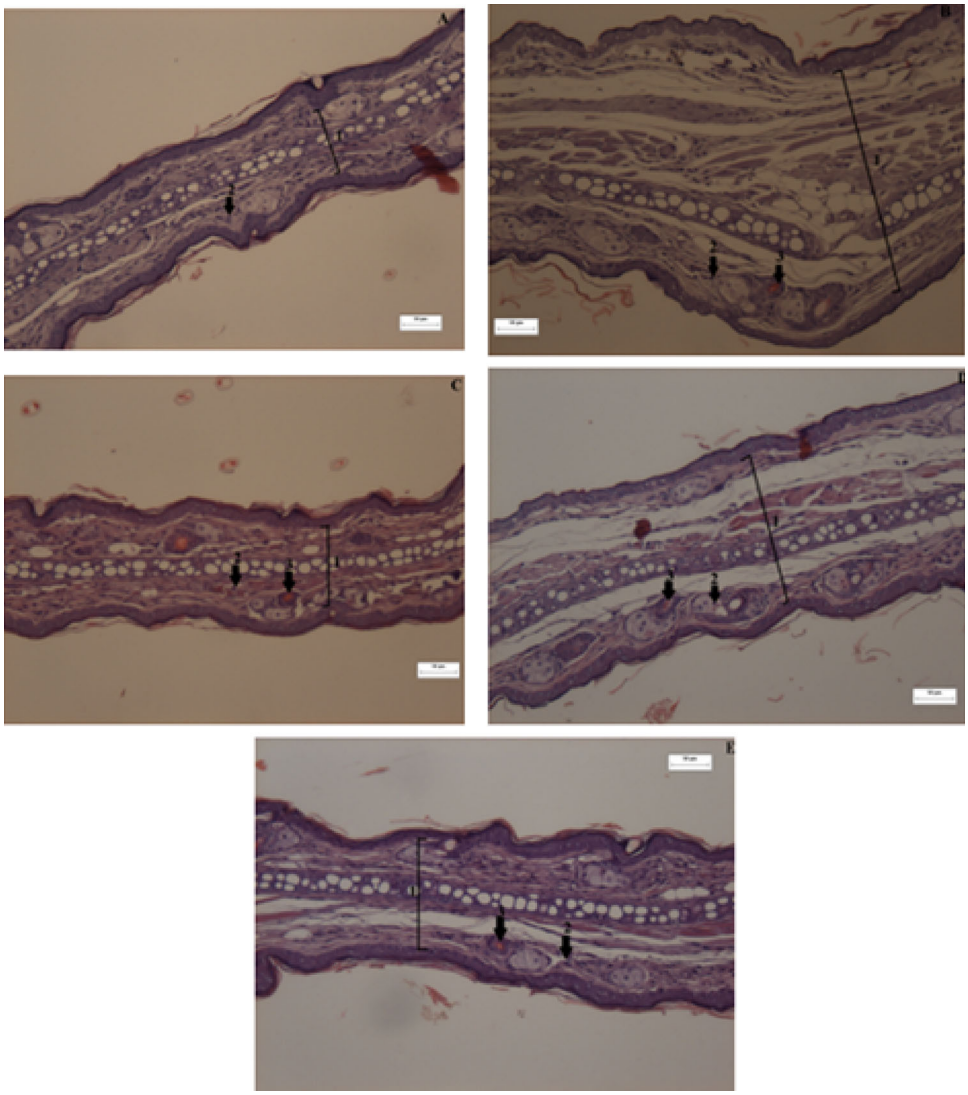

Fig. 8 Photomicrograph of transverse sections of H&E-stained mice ear tissue sensitized with topical single application of Croton oil examined under qualitative light microscopy (magnification: ×200, scale 50 μm). **a** Non-inflamed ears: left ear that received only acetone; **b** Negative control group: inflamed ear that received 20 μL of acetone; **c** Positive control group: inflamed ear that was treated with dexamethasone (0.1 %); **d** Inflamed ear that was treated with EEBP (0.25 %); **e** Inflamed ear that was treated with EEBP/βCD (0.5 %). The *number 1* indicates the ear thickness (edema). The *arrows* with *number 2* and *3* indicate inflammatory cells (infiltration of polymorphonuclear leucocytes) and blood vessels (vasodilation), respectively. The shown sections are representative of 7 animals per group, and images were captured through the Image-Pro® Plus software (version 6.0, Media Cybernetics, Inc., USA)

Table 1 Effect of formulation with EEBP and EEBP/βCD complex on ear edema thickness induced by Croton oil application

Group	Concentration	Ear thickness (μm)	Edema inhibition (%)
Non-inflamed	–	155.55 ± 20.14	–
Acetone (vehicle)	20 μL/ear	327.77 ± 15.33	0
EEBP	0.05 %	215.11 ± 41.8	34.37
	0.125 %	211.15 ± 24.5*	35.57*
	0.25 %	193.77 ± 6.46**	40.88**
EEBP/βCD phytocomplex	0.1 %	205.47 ± 18.22	37.31
	0.25 %	189.63 ± 7.41*	42.14*
	0.5 %	155.57 ± 5.72**	52.53**
Dexamethasone	0.1 %	118.54 ± 13.02	68.83

Values marked with (*) and (**) showed significant difference with $P < 0.01$

topical anti-inflammatory activity of several natural products [50]. Concerning to the traditional use of *B. pinnatum* for the treatment of skin disorders [19–21], the inhibitory effect of the topical formulations containing EEBP (0.05, 0.125 and 0.25 % w/w) and EEBP/βCD phytocomplex (0.1, 0.25 and 0.5 % w/w) on the increase of ear weight of male Swiss albino mice was assayed using Croton oil as irritant agent.

Our findings showed a significantly reduction ($P < 0.001$) of the ear edema when compared to the negative control group (34.06, 39.37 and 44.68 % for EEBP, and 35.31, 58.12 and 65.62 % for EEBP/βCD phytocomplex) (Fig. 6). This anti-inflammatory activity may be attributed to the synergism between anti-inflammatory and antioxidant compounds [21]. In addition, the presence of βCD or components of the anionic emulsion had no negative effect on anti-inflammatory activity of EEBP. As expected, dexamethasone (positive control), a steroidal anti-inflammatory drug, exerted elevated ear edema inhibition (75.62 %, $^{***}P < 0.001$).

When the inhibitory effect of the formulations containing EEBP and EEBP/βCD phytocomplex were compared among them, they were significantly ($^{\#\#}P < 0.01$) different in the inhibition of ear edema at concentrations of 0.125 and 0.25 % of EEBP and their corresponding 0.25 and 0.5 % of EEBP/βCD, showing that βCD enhanced the extent of EEBP anti-inflammatory action.

In order to evaluate the effect of βCD on the mechanism of cell infiltration resultant from anti-inflammatory process, the activity of myeloperoxidase (MPO) was measured in ear slices, since it is an indicative of a polymorphonuclear leukocytes influx [32, 33]. Figure 7 shows that EEBP and EEBP/βCD formulations significantly inhibited MPO activity induced by Croton oil when compared with the negative control ($^{***}P < 0.001$). These data also showed that the inhibition of MPO activity promoted by EEBP at concentrations of 0.125 and 0.25 % was significantly lower than EEBP/βCD complex at 0.25 and 0.50 % ($^{\#\#}P < 0.001$), reinforcing that βCD improved the anti-inflammatory effect of EEBP. In addition, the dexamethasone significantly inhibited the MPO responses in this model.

Histological analysis of the ear tissue clearly supported the results described above. Photomicrographs revealed that the edematous ears in untreated group (Fig. 8b, negative control) showed a significant increase of thickness at the dermis when compared to non-inflamed ears (Fig. 8a, basal). Expressive inflammatory cells (polymorphonuclear leukocytes) infiltration and vasodilatation were observed in the negative control group with the presence of connective tissue disruption and extracellular matrix fibers disorganization.

Figure 8d and e illustrate the effect of EEBP 0.25 % and EEBP/βCD 0.5 % formulations on reduction of all inflammatory parameters (ear thickness, inflammatory cells infiltration and vasodilation), when compared to the negative control group. As expected, dexamethasone produced the most pronounced effect in this model (Fig. 8c).

Table 1 presents the effect of EEBP and EEBP/βCD formulations on ear edema thickness where it was observed a significant difference ($P < 0.01$) among their inhibitory ability at concentrations of 0.125* and 0.25** % of EEBP and their corresponding 0.25* and 0.5** % of EEBP/βCD complex.

Based on the present results, it can be considered that the anti-inflammatory effect detected in the ear edema model induced by Croton oil (acute) involves the inhibition of arachidonic acid (AA) pathway with reduction of the vasodilatation, leukocyte infiltration and edema. This mechanistic hypothesis is supported by the presence of flavonoids in EEBP, previously reported in the literature [21] and corroborated by UV–Vis spectroscopic data. Flavonoids are important antioxidant agents that prevent the oxidative stress and inflammatory processes as demonstrated in the current study [21].

The improvement of anti-inflammatory activity of EEBP/βCD phytocomplex can be attributed to the presence of βCD, which increased the bioavailability of EEBP and caused the rise of solubility, thermal stability and different mechanisms of interaction with anionic emulsion. Moreover, inclusion complexes can accumulate in inflamed tissues through the formation of hydrogen bonds of hydroxyl cyclodextrins with cellular constituents, increasing the residence time and promoting a sustained release of the compound in the affected tissue [51].

Conclusion

In the present work, the phytocomplex composed by ethanolic extract of *B. pinnatum* complexated with βCD was incorporated in oil-in-water emulsion in order to produce a new semi-solid formulation. Physical–chemical analysis of the phytocomplex allowed to confirm the existence of interactions between βCD with components of the extract, such as flavonoids. Such interactions are responsible for hiding the fusion of the EEBP/βCD phytocomplex and to lead to the formation of lower and more stable nanostructures in water/ethanol solvent (98:2 v/v) than those observed for pure EEBP. Moreover, the interactions with βCD improved the in vitro antioxidant activity in two electrons transfer based reactions, which was thought to be due to the increase of the hydrogen-donating ability and increase of solubility of the extract components. Finally, through anti-inflammatory in vivo assays, it was possible to verify that topical application of EEBP/βCD semi-solid formulations significantly inhibited the ear edema when compared to the negative control group, as a result of potentiation of anti-inflammatory and anti-oxidant activities of EEBP by βCD, which provides greater bioavailability for extract components and greater ability to accumulate in inflamed tissues.

Acknowledgments The authors are grateful to the Fundação de Amparo à Pesquisa do Estado de Minas Gerais (FAPEMIG: APQ-

01243-10, APQ-00645-12, APQ-00435-14), Centro Federal de Educação Tecnológica de Minas Gerais (CEFET-MG), Conselho Nacional de Desenvolvimento Científico e Tecnológico (CNPq: 310175/2014-3, MCT/CNPq-NANO: 550321/2012-8), UFJF PROPESQ/PROPG/PROPLAN and Financiadora de Estudos e Pesquisas (FINEP: 0633/13) for financial support.

References

1. Bonifacio, B.V., da Silva, P.B., Ramos, M.A.D., Negri, K.M.S., Bauab, T.M., Chorilli, M.: Nanotechnology-based drug delivery systems and herbal medicines: a review. Int. J. Nanomed. **9**, 1–15 (2014)
2. Fang, Z.X., Bhandari, B.: Encapsulation of polyphenols—a review. Trends Food Sci Technol. **21**, 510–523 (2010)
3. Mourtzinos, I., Salta, F., Yannakopoulou, K., Chiou, A., Karathanos, V.T.: Encapsulation of olive leaf extract in beta-cyclodextrin. J. Agric. Food Chem. **55**, 8088–8094 (2007)
4. Mourtzinos, I., Makris, D.P., Yannakopoulou, K., Kalogeropoulos, N., Michali, I., Karathanos, V.T.: Thermal stability of anthocyanin extract of *Hibiscus sabdariffa* L. in the presence of beta-cyclodextrin. J. Agric. Food Chem. **56**, 10303–10310 (2008)
5. Kalogeropoulos, N., Konteles, S., Mourtzinos, I., Troullidou, E., Chiou, A., Karathanos, V.T.: Encapsulation of complex extracts in beta-cyclodextrin: an application to propolis ethanolic extract. J. Microencapsul. **26**, 603–613 (2009)
6. Spada, G., Gavini, E., Cossu, M., Rassu, G., Carta, A., Giunchedi, P.: Evaluation of the effect of hydroxypropyl-beta-cyclodextrin on topical administration of milk thistle extract. Carbohydr. Polym. **92**, 40–47 (2013)
7. De Sousa, F.B., Lima, A.C., Denadai, A.M.L., Anconi, C.P.A., De Almeida, W.B., Novato, W.T.G.: Superstructure based on beta-CD self-assembly induced by a small guest molecule. Phys. Chem. Chem. Phys. **14**, 1934–1944 (2012)
8. De Paula, W.X., Denadai, A.M., Santoro, M.M., Braga, A.N., Santos, R.A., Sinisterra, R.D.: Supramolecular interactions between losartan and hydroxypropyl-beta-CD: ESI mass-spectrometry, NMR techniques, phase solubility, isothermal titration calorimetry and anti-hypertensive studies. Int. J. Pharm. **404**, 116–123 (2011)
9. De Sousa, F.B., Denadai, A.M.L., Lula, I.S., Ianzer, D., Malaspina, E.R., de Camargo, A.C.M., et al.: Structural and physical-chemical evaluation of Bradykinin potentiating peptide and its high soluble supramolecular complex. J. Incl. Phenom. Macrocycl. Chem. **67**, 407–422 (2010)
10. Jensen, C.E., dos Santos, R.A., Denadai, A.M., Santos, C.F., Braga, A.N., Sinisterra, R.D.: Pharmaceutical composition of valsartan: beta-cyclodextrin: physico-chemical characterization and anti-hypertensive evaluation. Molecules **15**, 4067–4084 (2010)
11. Kurkov, S.V., Loftsson, T.: Cyclodextrins. Int. J. Pharm. **453**, 167–180 (2013)
12. Rocks, N., Bekaert, S., Coia, I., Paulissen, G., Gueders, M., Evrard, B., et al.: Curcumin-cyclodextrin complexes potentiate gemcitabine effects in an orthotopic mouse model of lung cancer. Br. J. Cancer **107**, 1083–1092 (2012)
13. Zhao, M.M., Wang, H.Y., Yang, B., Tao, H.: Identification of cyclodextrin inclusion complex of chlorogenic acid and its antimicrobial activity. Food Chem. **120**, 1138–1142 (2010)
14. Monti, D., Tampucci, S., Chetoni, P., Burgalassi, S., Saino, V., Centini, M., Staltari, L., Anselmi, C.: Permeation and distribution of ferulic acid and its alpha-cyclodextrin complex from different formulations in hairless rat skin. AAPS PharmSciTech. **12**, 514–520 (2011)
15. Li, X.D., Li, H., Liu, M., Li, G.Q., Li, L.W., Sun, D.Z.: From guest to ligand—a study on the competing interactions of anti-tumor drug resveratrol with beta-cyclodextrin and bovine serum albumin. Thermochim. Acta **521**, 74–79 (2011)
16. Folch-Cano, C., Guerrero, J., Speisky, H., Jullian, C., Olea-Azar, C.: NMR and molecular fluorescence spectroscopic study of the structure and thermodynamic parameters of EGCG/beta-cyclodextrin inclusion complexes with potential antioxidant activity. J. Incl. Phenom. Macrocycl. Chem. **78**, 287–298 (2014)
17. Kalogeropoulos, N., Konteles, S.J., Troullidou, E., Mourtzinos, I., Karathanos, V.T.: Chemical composition, antioxidant activity and antimicrobial properties of propolis extracts from Greece and Cyprus. Food Chem. **116**, 452–461 (2009)
18. Biswas, S.K., Chowdhury, A., Das, J., Hosen, S.M.Z., Uddin, R., Rahaman, M.S.: Literature review on pharmacological potentials of Kalanchoe pinnata (Crassulaceae). Afr. J. Pharm. Pharmacol. **5**, 1258–1262 (2011)
19. Prasad, A.K., Kumar, S., Iyer, S.V., Sudani, R.J., Vaidya, S.K.: Pharmacognostical, phytochemical and pharmacological review on Bryophyllum pinnata. Int. J. Pharm. Biol. Arch. **3**, 423–433 (2012)
20. Milad, R., El-Ahmady, S., Singab, A.N.: Genu Kalanchoe (Crassulaceae): a review of its ethomedicial, botanical, chemical and pharmacological properties. Eur. J. Med. Plants **4**, 86–104 (2014)
21. Chibli, L.A., Rodrigues, K.C.M., Gasparetto, C.M., Pinto, N.C.C., Fabri, R.L., Scio, E., Alves, M.S., Del-Vechio-Vieira, G., Sousa, O.V.: Anti-inflammatory effects of *Bryophyllum pinnatum* (Lam.) Oken ethanol extract in acute and chronic cutaneous inflammation. J. Ethnopharmacol. **154**, 330–338 (2014)
22. Afzal, M., Gupta, G., Kazmi, I., Rahman, M., Afzal, O., Alam, J., Hakeem, K.R., Pravez, M., Gupta, R., Anwar, F.: Anti-inflammatory and analgesic potential of a novel steroidal derivative from *Bryophyllum pinnatum*. Fitoterapia **83**, 853–858 (2012)
23. Okwu, D.E., Josiah, C.: Evaluation of the chemical composition of two Nigerian medicinal plants. Afr. J. Biotech. **5**, 357–361 (2006)
24. Ozdemir, N., Erkin, J.: Enhancement of dissolution rate and bioavailability of sulfamethoxazole by complexation with beta-cyclodextrin. Drug Dev. Ind. Pharm. **38**, 331–340 (2012)
25. Whang, H.S., Tonelli, A.: Release characteristics of the non-toxic insect repellant 2-undecanone from its crystalline inclusion compound with alpha-cyclodextrin. J. Incl. Phenom. Macrocycl. Chem. **62**, 127–134 (2008)
26. Fan, Y.X., Li, J.F., Dong, C.A.: Preparation and study on the inclusion complexes of two tanshinone compounds with beta-cyclodextrin. Spectrochim. Acta A **61**, 135–140 (2005)
27. Xu, R.L.: Methods to resolve mobility from electrophoretic laser-light scattering measurement. Langmuir **9**, 2955–2962 (1993)
28. Mensor, L.L., Menezes, F.S., Leitao, G.G., Reis, A.S., dos Santos, T.C., Coube, C.S., Leitao, S.G.: Screening of Brazilian plant extracts for antioxidant activity by the use of DPPH free radical method. Phytother. Res. **15**, 127–130 (2001)
29. Oyaizu, M.: Antioxidative activities of browning products of glucosamine fractionated by organic-solvent and thin-layer chromatography. J. Jpn. Soc. Food Sci. **35**, 771–775 (1988)
30. Oyaizu, M.: Effects of amino-acids, organic-acids or sugars on antioxidative activity of browning products prepared from glucosamine. J. Jpn. Soc. Food Sci. **35**, 846–850 (1988)
31. Schiantarelli, P., Cadel, S., Acerbi, D., Pavesi, L.: Anti-inflammatory activity and bioavailability of percutaneous piroxicam. Drug Res. **32–1**, 230–235 (1982)
32. Deyoung, L.M., Kheifets, J.B., Ballaron, S.J., Young, J.M.: Edema and cell infiltration in the phorbol ester-treated mouse ear are temporally separate and can be differentially modulated by pharmacologic agents. Agents Actions **26**, 335–341 (1989)

33. Bradley, P.P., Priebat, D.A., Christensen, R.D., Rothstein, G.: Measurement of cutaneous inflammation—estimation of neutrophil content with an enzyme marker. J. Invest. Dermatol. **78**, 206–209 (1982)
34. Lowry, O.H., Rosebrough, N.J., Farr, A.L., Randall, R.J.: Protein measurement with the folin phenol reagent. J. Biol. Chem. **193**, 265–275 (1951)
35. Sargent, M.G.: Fiftyfold amplification of the lowry protein assay. Anal. Biochem. **163**, 476–481 (1987)
36. Egyed, O.: Spectroscopic studies on beta-cyclodextrin. Vib. Spectrosc. **1**, 225–227 (1990)
37. Heneczkowski, M., Kopacz, M., Nowak, D., Kuzniar, A.: Infrared spectrum analysis of some flavonoids. Acta Pol. Pharm. **58**, 415–420 (2001)
38. Azemin, A., Dharmaraj, S., Hamdan, M.R., Mat, N., Ismail, Z., Mohd, K.S.: Discriminating *Ficus deltoidea* var. bornensis from different localities by HPTLC and FTIR fingerprinting. J. Appl. Pharm. Sci. **4**, 69–75 (2014)
39. Silverstein, R.M., Bassler, C.G., Morrill, T.C.: Spectrometric Identification of Organic Compounds, 5th edn. Wiley, New York (1991)
40. Stalikas, C.D.: Extraction, separation, and detection methods for phenolic acids and flavonoids. J. Sep. Sci. **30**, 3268–3295 (2007)
41. Cotton, T.M., Trifunac, A.D., Ballschm, K., Katz, J.J.: State of chlorophyll a in vitro and in vivo from electronic-transition spectra, and nature of antenna chlorophyll. Biochim. Biophys. Acta **368**, 181–198 (1974)
42. Giordano, F., Novak, C., Moyano, J.R.: Thermal analysis of cyclodextrins and their inclusion compounds. Thermochim. Acta **380**, 123–151 (2001)
43. Denadai, A.M.L., Santoro, M.M., Lopes, M.T.P., Chenna, A., de Sousa, F.B., Avelar, G.M., et al.: A supramolecular complex between proteinases and beta-cyclodextrin that preserves enzymatic activity—physicochemical characterization. Biodrugs **20**, 283–291 (2006)
44. Marini, A., Berbenni, V., Bruni, G., Massarotti, V., Mustarelli, P., Villa, M.: Dehydration of the cyclodextrins—a model system for the interactions of biomolecules with water. J. Chem. Phys. **103**, 7532–7540 (1995)
45. Agostiano, A., Catucci, L., Cosma, P., Fini, P.: Aggregation processes and photophysical properties of chlorophyll a in aqueous solutions modulated by the presence of cyclodextrins. Phys. Chem. Chem. Phys. **5**, 2122–2128 (2003)
46. Lopez-Leon, T., Gea-Jodar, P.M., Bastos-Gonzalez, D., Ortega-Vinuesa, J.L.: Hofmeister effects in the restabilization of IgG–latex particles: testing Ruckenstein's theory. Langmuir **21**, 87–93 (2005)
47. Yang, J.X., Guo, J., Yuan, J.F.: In vitro antioxidant properties of rutin. LWT Food Sci. Technol. **41**, 1060–1066 (2008)
48. Lue, B.M., Nielsen, N.S., Jacobsen, C., Hellgren, L., Guo, Z., Xu, X.B.: Antioxidant properties of modified rutin esters by DPPH, reducing power, iron chelation and human low density lipoprotein assays. Food Chem. **123**, 221–230 (2010)
49. Barnes, H.A., Hutton, J.F., Walters, K.: An Introduction to Rheology, 5th edn. Elsevier, Amsterdam (1998)
50. Phanse, M.A., Manohar, J.P., Abbulu, K., Chaudhari, P.D., Pate, B.: In-vivo and in vitro screening of medicinal plants for their anti-inflammatory activity: an overview. J. App. Pharm. Sci. **2**, 19–33 (2012)
51. Alves, M.P., Scarrone, A.L., Santos, M., Pohlmann, A.R., Guterres, S.S.: Human skin penetration and distribution of nimesulide from hydrophilic gels containing nanocarriers. Int. J. Pharm. **341**, 215–220 (2007)